Supporting Information

Inclusion Complexation and Self-association of Cucurbit[*n*]uril (*n* = 6, 7) and Diquat under Pseudo-physiological Conditions

Hiroyuki Tsutsumi,* Tomonori Ohata, Rie Nakashima, Hirohito Ikeda

Faculty of Pharmaceutical Sciences, Fukuoka University; 8-19-1 Nanakuma, Jonan-ku, Fukuoka-shi, Fukuoka, 814-0180, Japan

*To whom correspondence should be addressed. E-mail: h-tsutsumi@fukuoka-u.ac.jp

Table of Contents

qNMR spectra were recorded over a spectral width of 12000 Hz using 8 scans without spinning. The pulse angle is 90°, and the repetition time is 64 s. DSS-d_6 (FUJIFILM Wako Chemicals Co) is used as an internal reference in qNMR. CB[6] or CB[7] were dissolved in NaCl-D_2O. Purities of CB[6] or CB[7] were calculated using integrated values of the methyl proton signal of the trimethylsilyl group of DSS-d_6 (Si-CH_3) and the H^a and H^c proton signals of CB[6] or CB[7]. In the case of CB[7], although DSS-d_6 forms the complex with CB[7], the integration value of Si-CH_3 did not affect on the quantitative (-0.744 ppm). Purities of CB[6] or CB[7] were 82.9 % and 87.2 %, respectively.

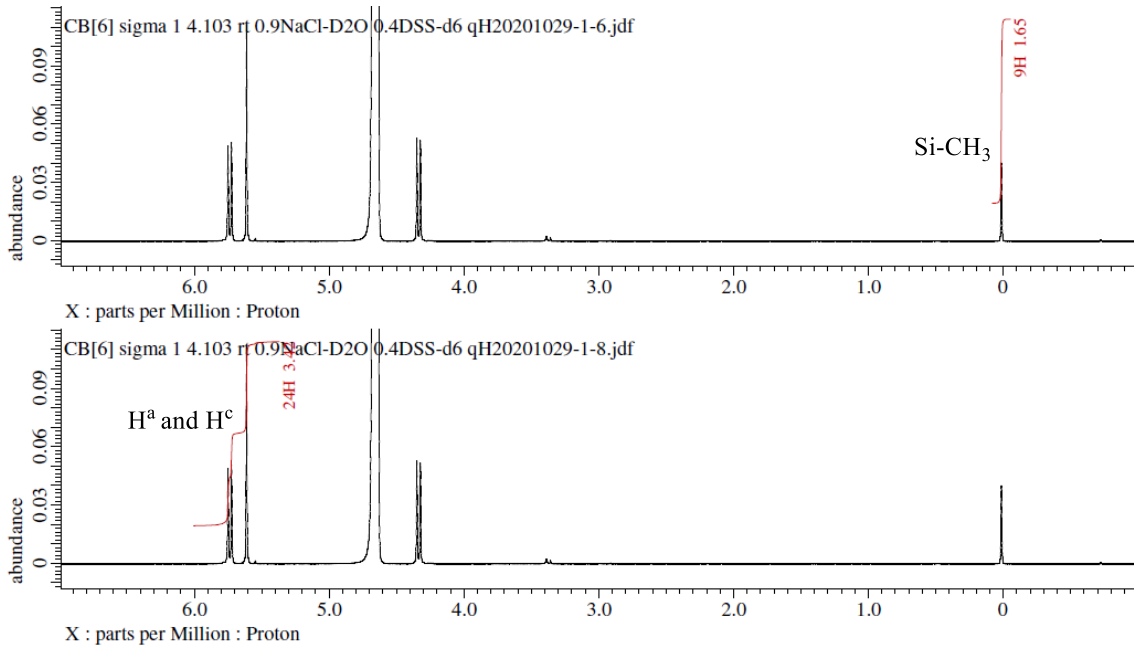

Fig. S1 qNMR spectra of CB[6].

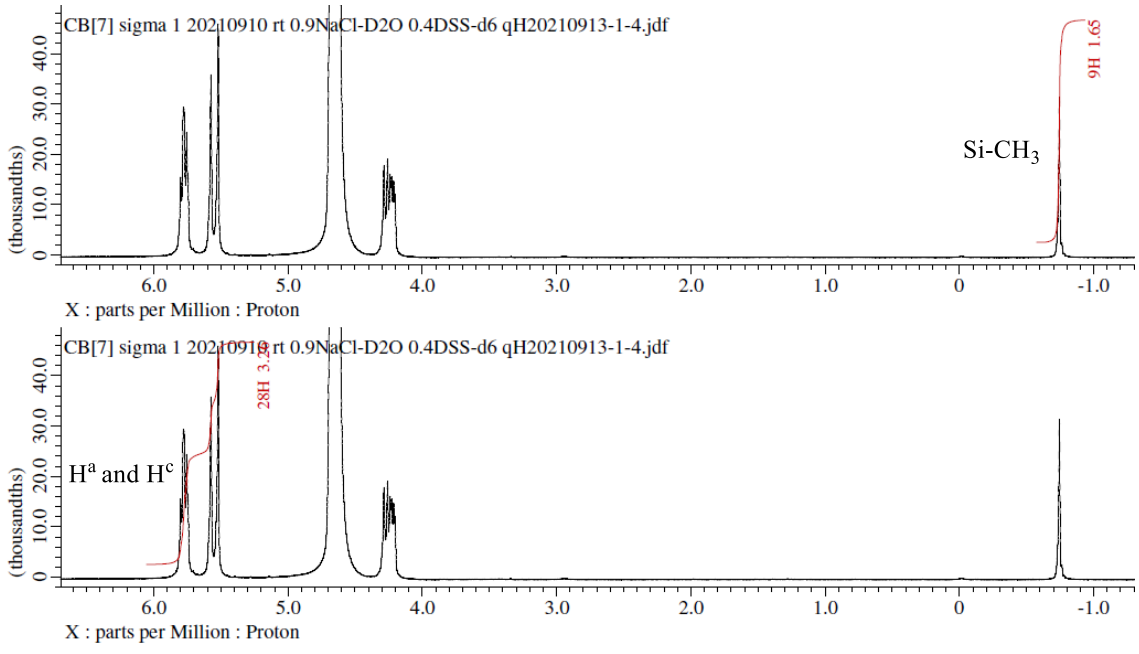

Fig. S2 qNMR spectra of CB[7].

The stoichiometry for the inclusion complexation of CB[7] and DQ was investigated via Job's plot by using ^{1}H NMR measurement when the sum of the CB[7] and DQ concentrations ([CB[7]] and [DQ]) was maintained at 1 and 10 mM; changes in the observed chemical shift ($\Delta\delta_{obs}$) of the DQ H^4 proton signal were used, and the stoichiometry was found from the plot of the $\Delta\delta_{obs}$*[DQ] as function of the ratio [DQ]/([CB[7]] + [DQ]).

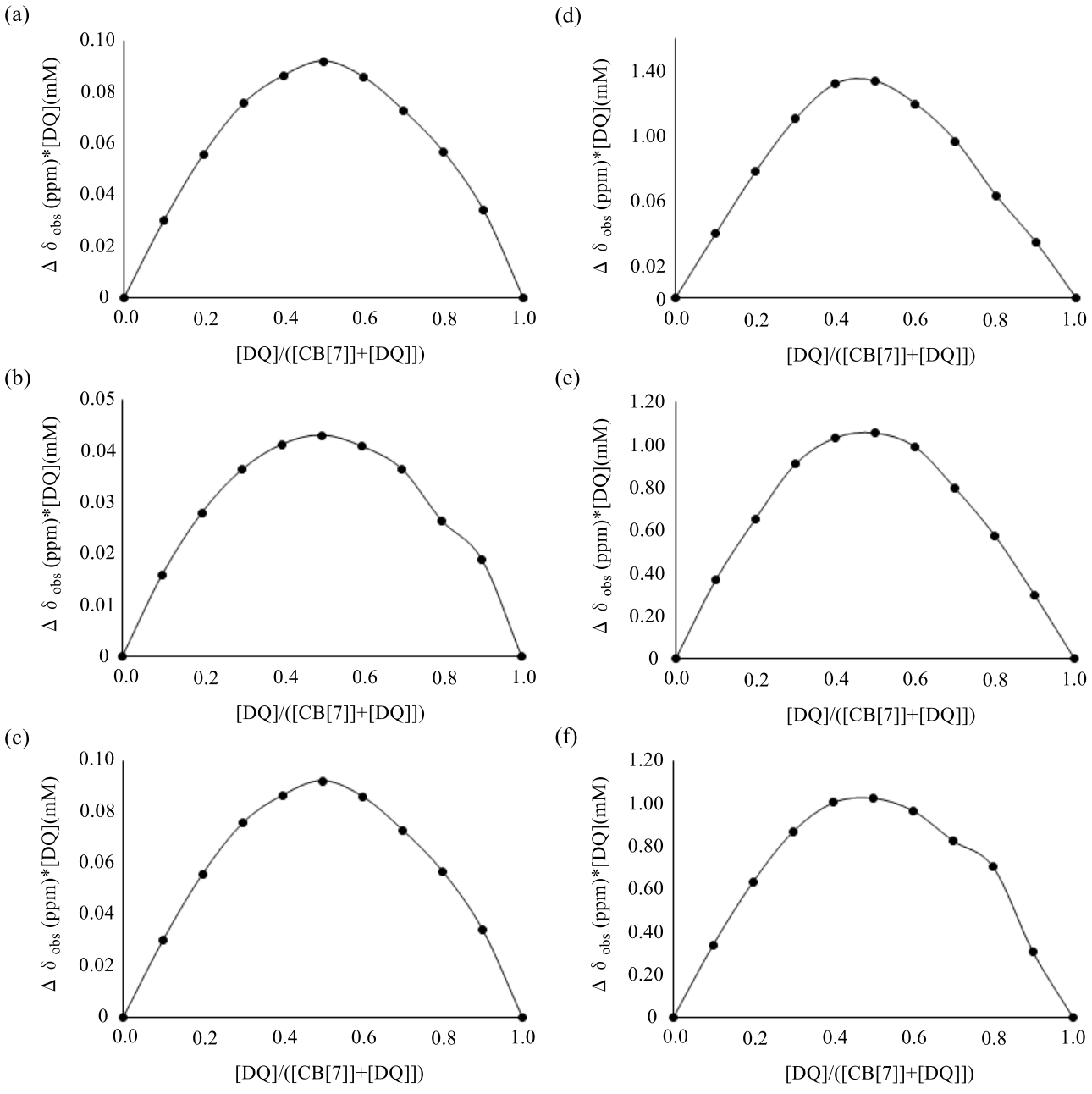

Fig. S3 Continuous variation plot (Job's plot) by using ^{1}H NMR measurement for the inclusion complexation of CB[7] and DQ: total concentration 1 mM in (a) pD1.2, (b) pD7.4, and (c) NaCl-D_2O; total concentration 10 mM in (d) pD1.2, (e) pD7.4, and (f) NaCl-D_2O.

The stoichiometry and association constant for the inclusion complexation between CB[7] and DQ were calculated via regression analysis at 30 - 65 °C in pD1.2, pD7.4, and NaCl-D_2O (Fig. S3, S5, and S7) while continuously increasing the CB[7] concentration ([CB[7]) from 0 to 5 mM in a constant concentration of DQ ([DQ]; 0.5 mM). The following Eqn (1) was used for regression analysis. K and n are, respectively, the association constant and stoichiometry of CB[7] and DQ, $\Delta\delta_{obs}$ means ($\delta_{DQ} - \delta_{obs}$), $\Delta\delta_{CX}$ indicates ($\delta_{DQ} - \delta_{CX}$), and δ_{DQ}, δ_{CX}, and δ_{obs} are the chemical shifts (in ppm) of the H^4 protons of, correspondingly, DQ in a free state, the CB[7]-DQ inclusion complex, and the CB[7]-DQ mixture in the ^{1}H NMR spectra. In Fig. S3, S5, and S7, m1, m2, and m3 indicate that $\Delta\delta_{CX}$, K, and n, respectively. The thermodynamic parameters, that is, free energy change (ΔG), enthalpy change (ΔH), and entropy change (ΔS), for the inclusion complexation of CB[7] and DQ were derived from Van't Hoff plots by using association constants.

$$n\ \mathrm{CB[7]} + \mathrm{DQ} \underset{}{\overset{K}{\rightleftharpoons}} \mathrm{CB[7]\text{-}DQ}$$

$$[\mathrm{CB[7]}] = \left[\frac{1}{\left(\frac{\Delta\ \delta_{cx}}{\Delta\ \delta_{obs}} - 1 \right) K} \right]^{1/n} + n \frac{\Delta\ \delta_{obs}}{\Delta\ \delta_{cx}} [\mathrm{DQ}] \quad \cdots\cdot \mathrm{Eqn\ (1)}$$

(a)

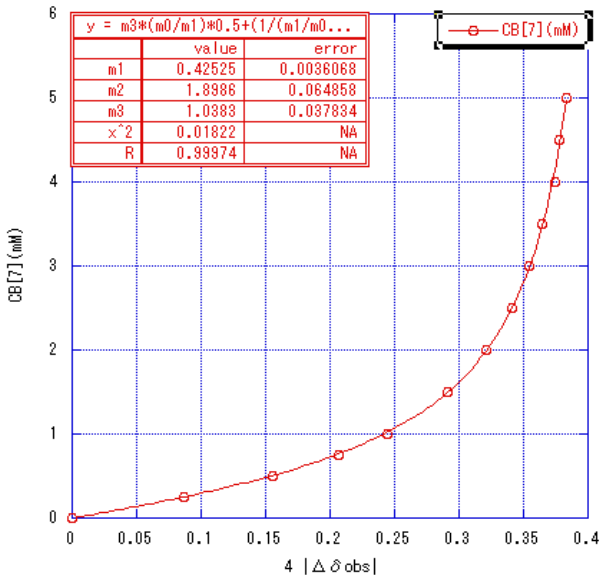
CB[7]-DQ 30 H4
y = m3*(m0/m1)*0.5+(1/(m1/m0...
CB[7](mM)
value error
m1 0.42525 0.0036068
m2 1.8986 0.064858
m3 1.0383 0.037834
x^2 0.01822 NA
R 0.99974 NA
CB[7](mM)
4 |Δδobs|

(b)

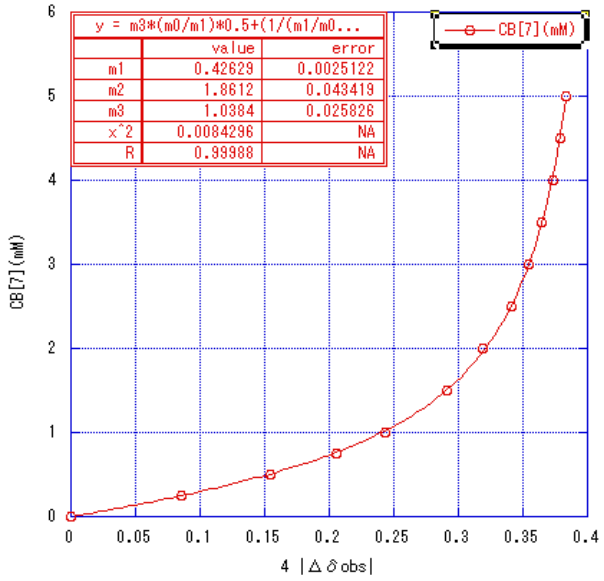
CB[7]-DQ 35 H4
y = m3*(m0/m1)*0.5+(1/(m1/m0...
CB[7](mM)
value error
m1 0.42629 0.0025122
m2 1.8612 0.043419
m3 1.0384 0.025826
x^2 0.0084236 NA
R 0.99988 NA
CB[7](mM)
4 |Δδobs|

(c)

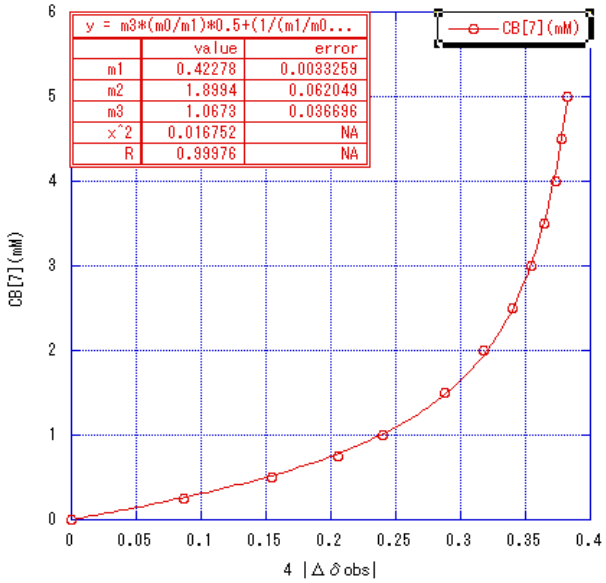
CB[7]-DQ 40 H4
y = m3*(m0/m1)*0.5+(1/(m1/m0...
CB[7](mM)
value error
m1 0.42278 0.0033259
m2 1.8994 0.062049
m3 1.0673 0.036696
x^2 0.016752 NA
R 0.99976 NA
CB[7](mM)
4 |Δδobs|

(d)

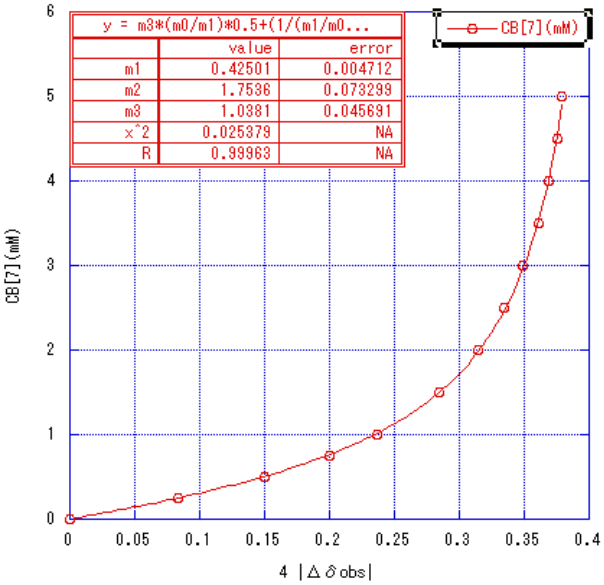
CB[7]-DQ 45 H4
y = m3*(m0/m1)*0.5+(1/(m1/m0...
CB[7](mM)
value error
m1 0.42501 0.004712
m2 1.7536 0.073299
m3 1.0381 0.045691
x^2 0.025379 NA
R 0.99963 NA
CB[7](mM)
4 |Δδobs|

(e)

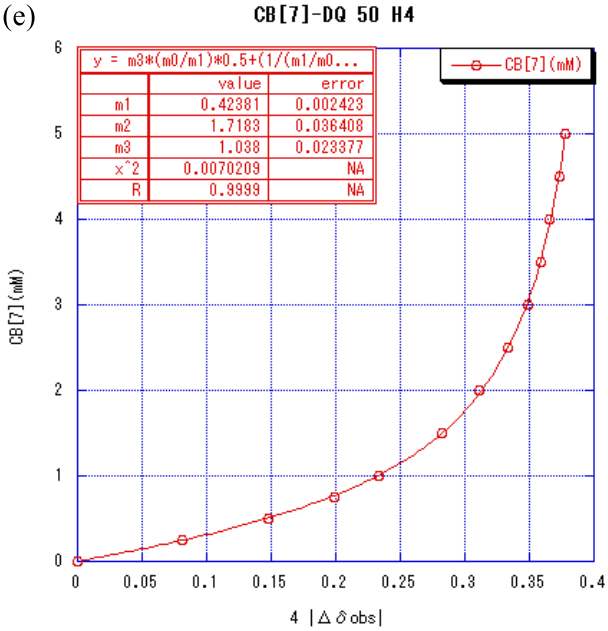
CB[7]-DQ 50 H4
y = m3*(m0/m1)*0.5+(1/(m1/m0...
CB[7](mM)
value error
m1 0.42381 0.002423
m2 1.7183 0.036408
m3 1.038 0.023377
x^2 0.0070209 NA
R 0.9999 NA
CB[7](mM)
4 |Δδobs|

(f)

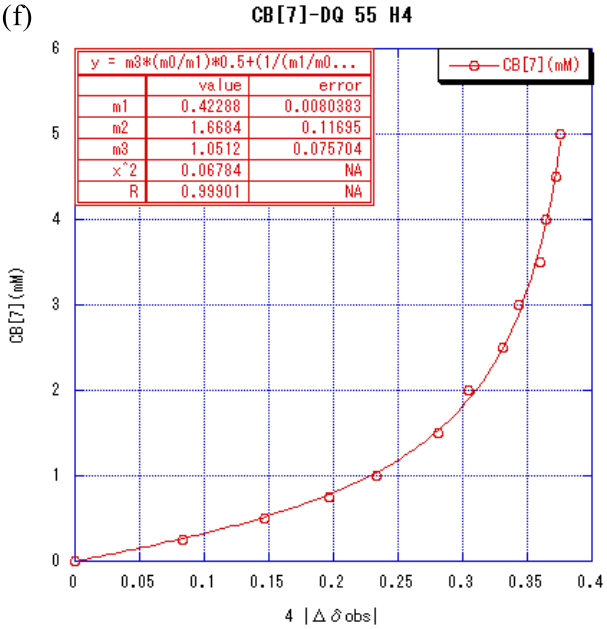
CB[7]-DQ 55 H4
y = m3*(m0/m1)*0.5+(1/(m1/m0...
CB[7](mM)
value error
m1 0.42288 0.0080383
m2 1.6684 0.11695
m3 1.0512 0.075704
x^2 0.06784 NA
R 0.99901 NA
CB[7](mM)
4 |Δδobs|

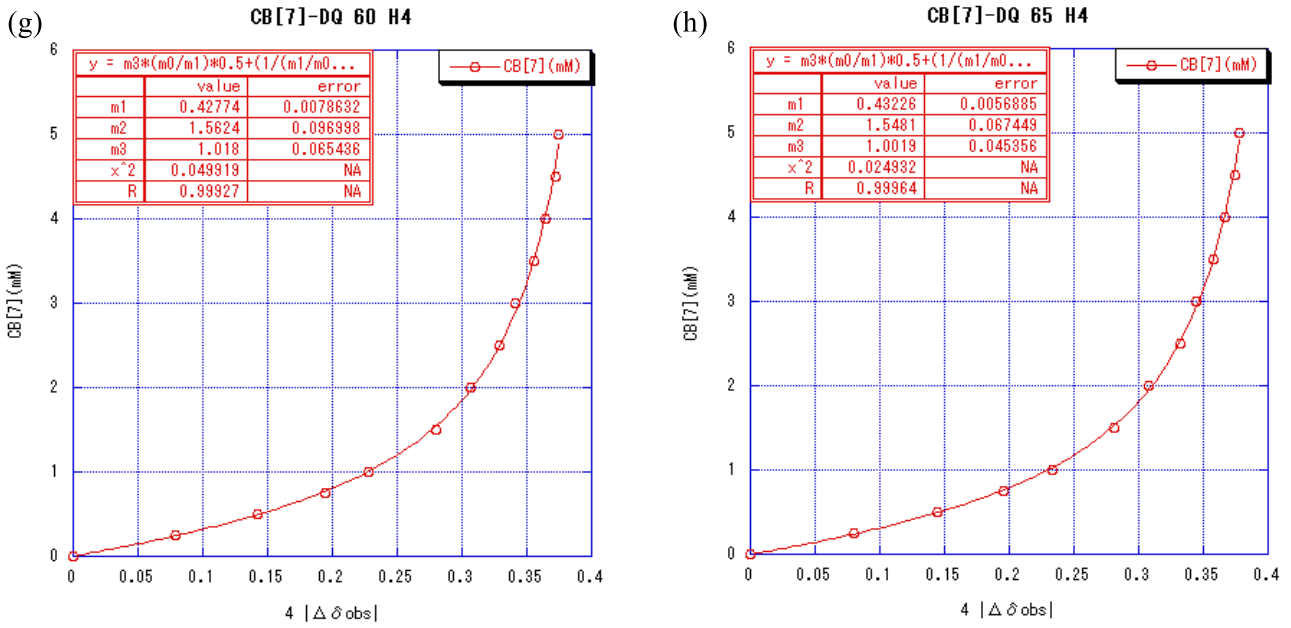

Fig. S4 Regression analysis by using Eqn (1) based on $\Delta\delta_{obs}$ of the H^4 proton signal of DQ (0.5 mM DQ) at 30 - 65 °C in pD1.2: (a) 30 °C, (b) 35 °C, (c) 40 °C, (d) 45 °C, (e) 50 °C, (f) 55 °C, (g) 60 °C, and (h) 65 °C.

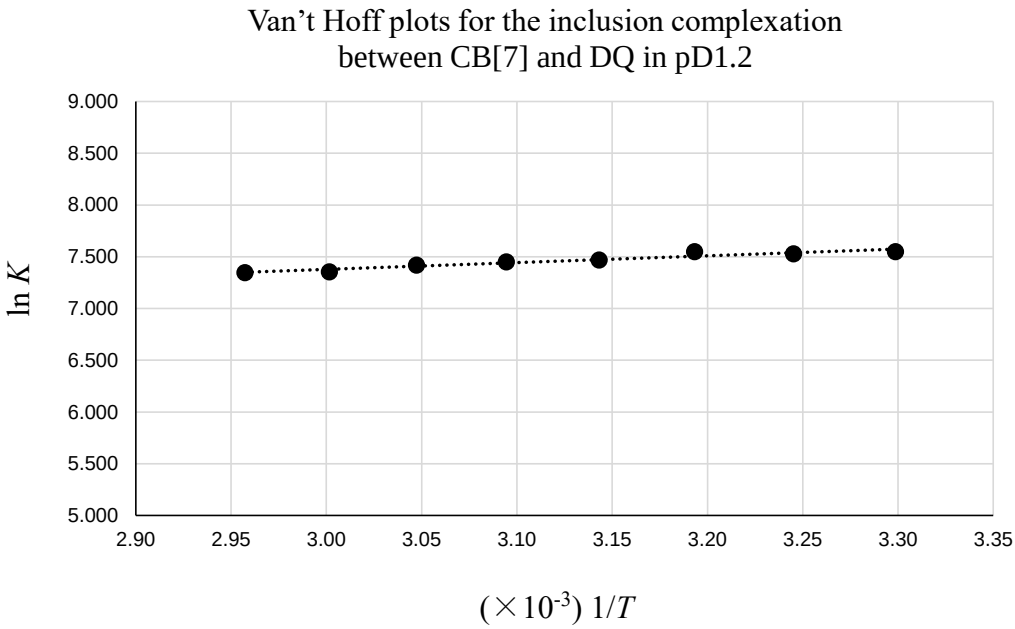

Fig. S5 Van't Hoff plots for the inclusion complexation between CB[7] and DQ (0.5 mM DQ) in pD1.2.

(a)

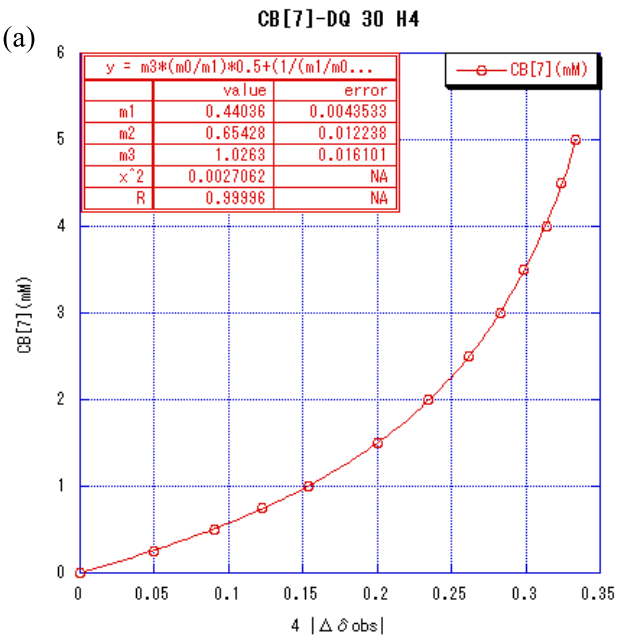
CB[7]-DQ 30 H4
y = m3*(m0/m1)*0.5+(1/(m1/m0...
CB[7](mM)
value error
m1 0.44036 0.0043533
m2 0.65428 0.012238
m3 1.0263 0.016101
x^2 0.0027062 NA
R 0.99996 NA
CB[7](mM)
4 |Δδobs|

(b)

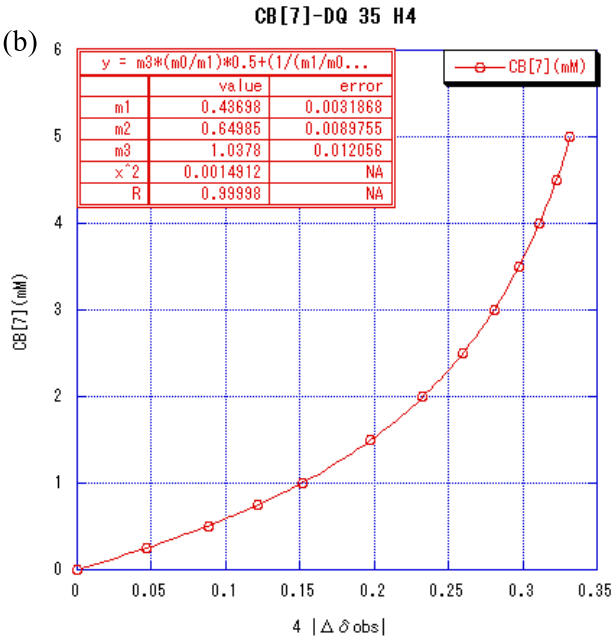
CB[7]-DQ 35 H4
y = m3*(m0/m1)*0.5+(1/(m1/m0...
CB[7](mM)
value error
m1 0.43698 0.0031868
m2 0.64985 0.0089755
m3 1.0378 0.012056
x^2 0.0014912 NA
R 0.99998 NA
CB[7](mM)
4 |Δδobs|

(c)

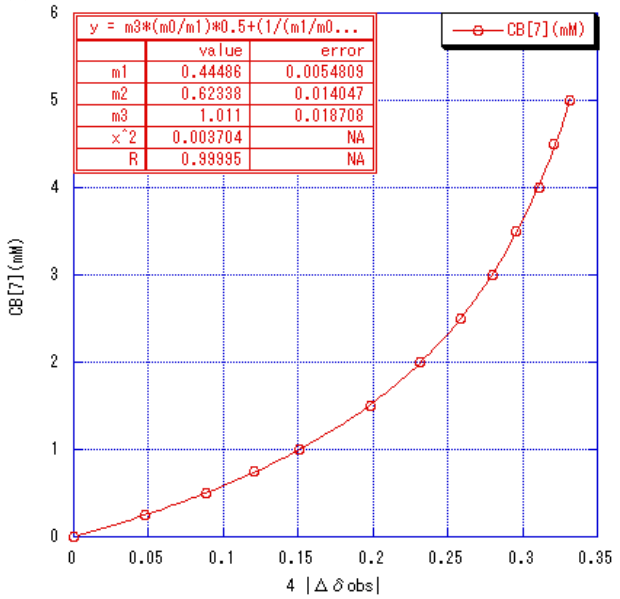
CB[7]-DQ 40 H4
y = m3*(m0/m1)*0.5+(1/(m1/m0...
CB[7](mM)
value error
m1 0.44486 0.0054809
m2 0.62338 0.014047
m3 1.011 0.018708
x^2 0.003704 NA
R 0.99995 NA
CB[7](mM)
4 |Δδobs|

(d)

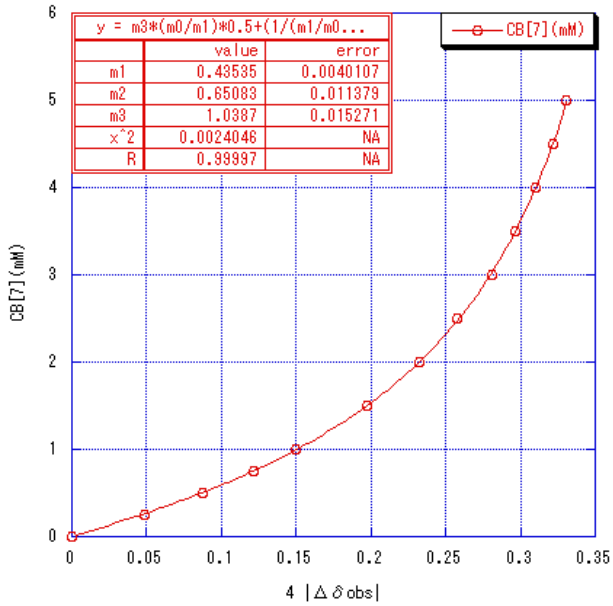
CB[7]-DQ 45 H4
y = m3*(m0/m1)*0.5+(1/(m1/m0...
CB[7](mM)
value error
m1 0.43535 0.0040107
m2 0.65083 0.011379
m3 1.0387 0.015271
x^2 0.0024046 NA
R 0.99997 NA
CB[7](mM)
4 |Δδobs|

(e)

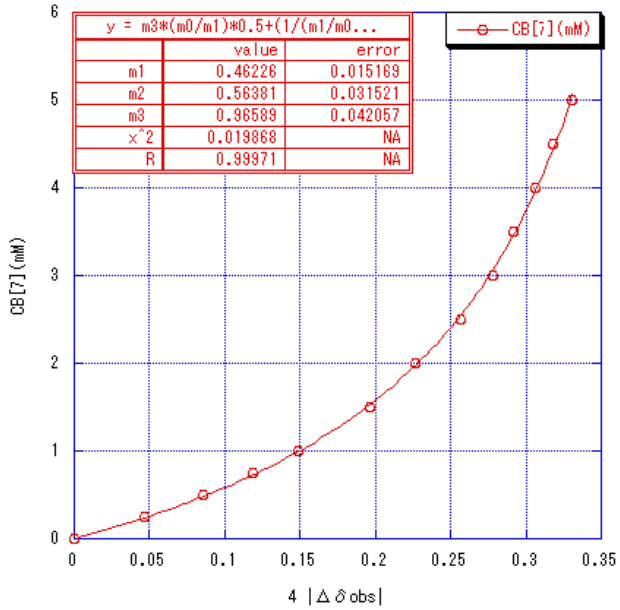
CB[7]-DQ 50 H4
y = m3*(m0/m1)*0.5+(1/(m1/m0...
CB[7](mM)
value error
m1 0.46226 0.015169
m2 0.56381 0.031521
m3 0.96589 0.042057
x^2 0.019868 NA
R 0.99971 NA
CB[7](mM)
4 |Δδobs|

(f)

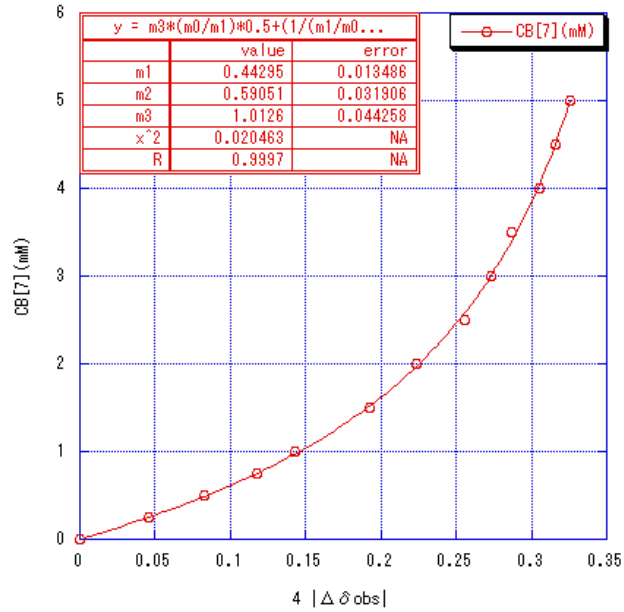
CB[7]-DQ 55 H4
y = m3*(m0/m1)*0.5+(1/(m1/m0...
CB[7](mM)
value error
m1 0.44295 0.013486
m2 0.59051 0.031906
m3 1.0126 0.044258
x^2 0.020463 NA
R 0.9997 NA
CB[7](mM)
4 |Δδobs|

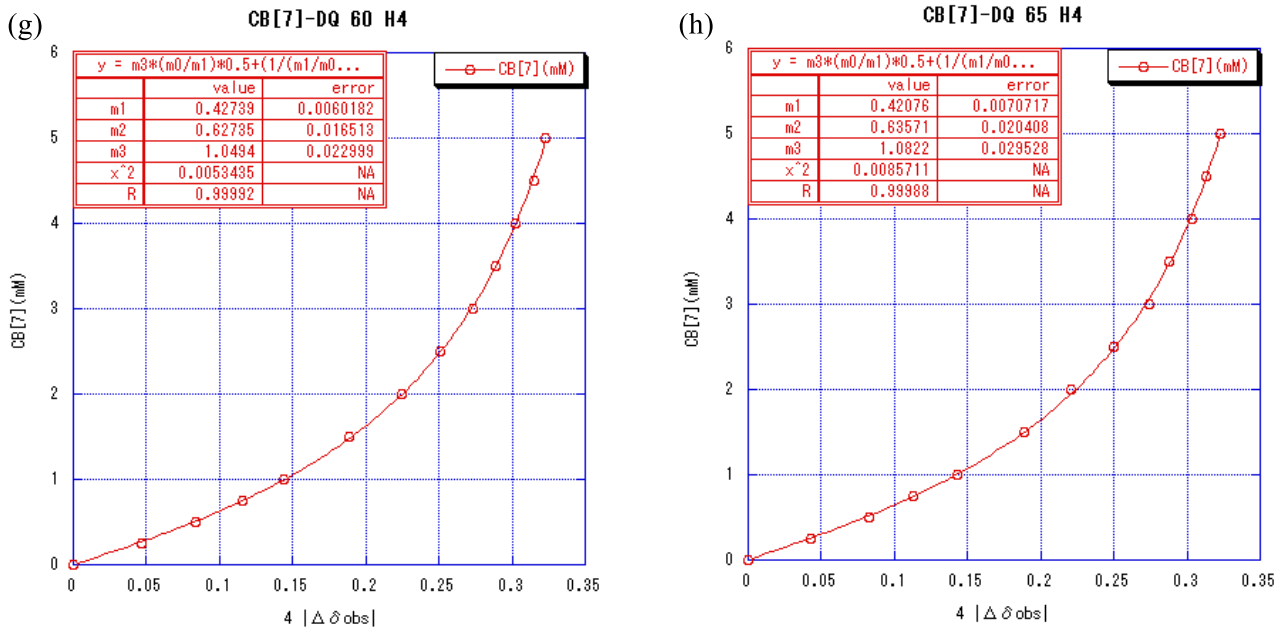

Fig. S6 Regression analysis by using Eqn (1) based on $\Delta\delta_{obs}$ of the H^4 proton signal of DQ (0.5 mM DQ) at 30 - 65 °C in pD7.4: (a) 30 °C, (b) 35 °C, (c) 40 °C, (d) 45 °C, (e) 50 °C, (f) 55 °C, (g) 60 °C, and (h) 65 °C.

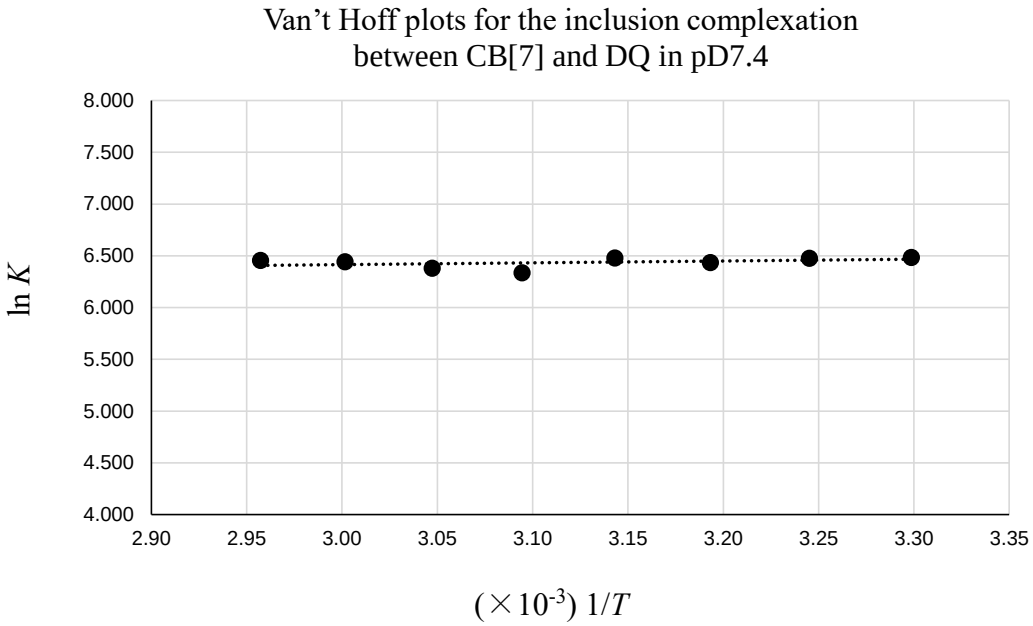

Fig. S7 Van't Hoff plots for the inclusion complexation between CB[7] and DQ (0.5 mM DQ) in pD7.4.

(a)

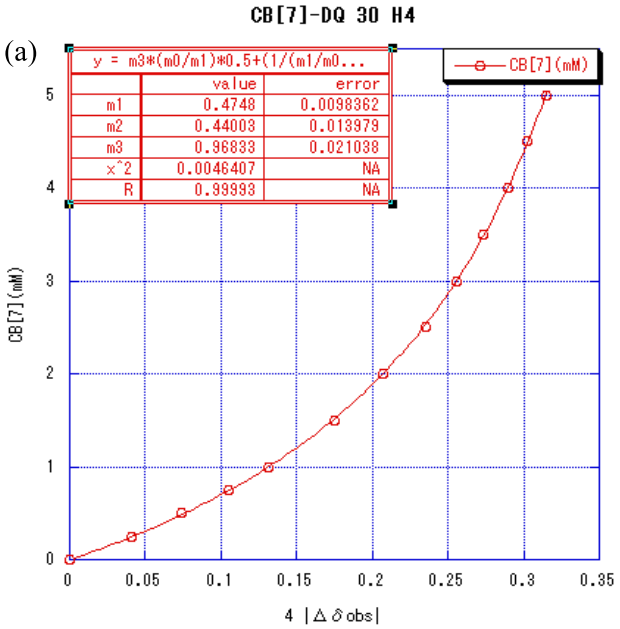
CB[7]-DQ 30 H4
y = m3*(m0/m1)*0.5+(1/(m1/m0...
CB[7](mM)
value error
m1 0.4748 0.0098362
m2 0.44003 0.013979
m3 0.96833 0.021038
x^2 0.0046407 NA
R 0.99993 NA
CB[7](mM)
4 |Δδobs|

(b)

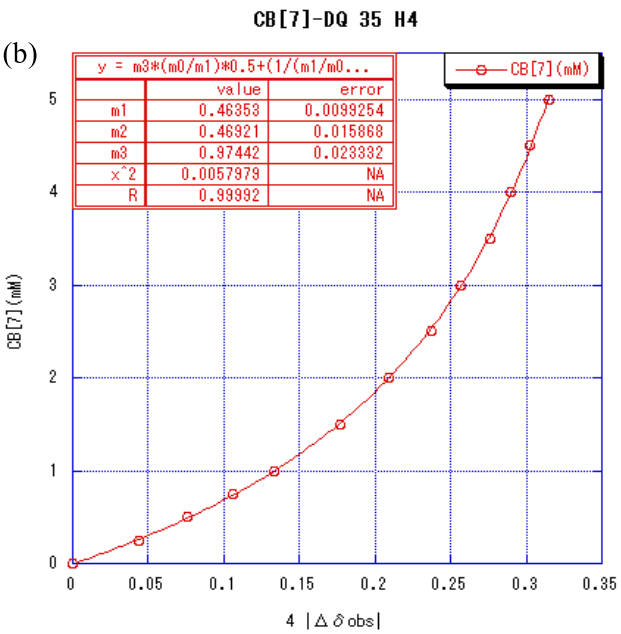
CB[7]-DQ 35 H4
y = m3*(m0/m1)*0.5+(1/(m1/m0...
CB[7](mM)
value error
m1 0.46353 0.0099254
m2 0.46921 0.015868
m3 0.97442 0.023332
x^2 0.0057979 NA
R 0.99992 NA
CB[7](mM)
4 |Δδobs|

(c)

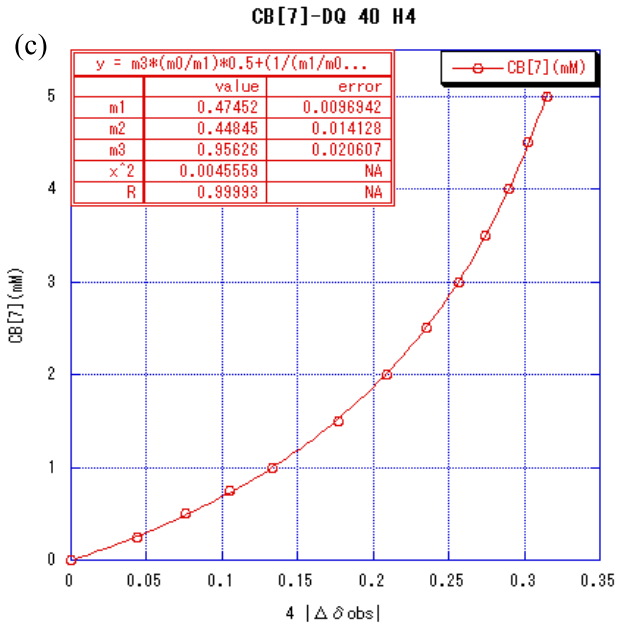
CB[7]-DQ 40 H4
y = m3*(m0/m1)*0.5+(1/(m1/m0...
CB[7](mM)
value error
m1 0.47452 0.0096942
m2 0.44845 0.014128
m3 0.95626 0.020607
x^2 0.0045559 NA
R 0.99993 NA
CB[7](mM)
4 |Δδobs|

(d)

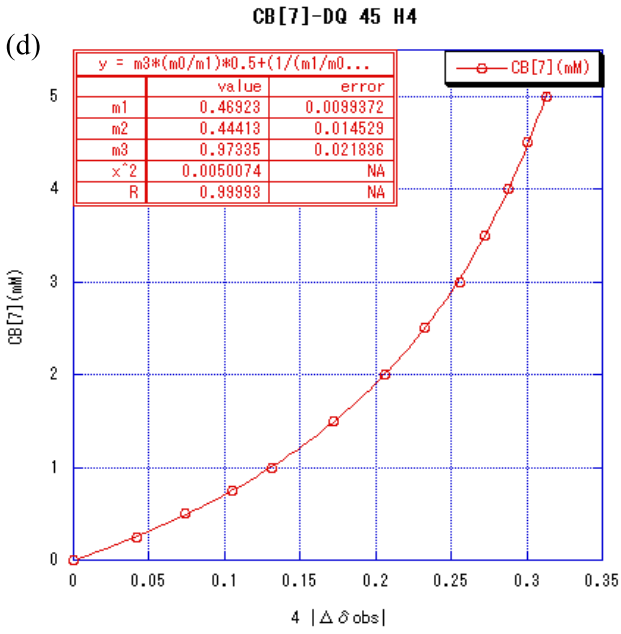
CB[7]-DQ 45 H4
y = m3*(m0/m1)*0.5+(1/(m1/m0...
CB[7](mM)
value error
m1 0.46923 0.0099372
m2 0.44413 0.014529
m3 0.97335 0.021836
x^2 0.0050074 NA
R 0.99993 NA
CB[7](mM)
4 |Δδobs|

(e)

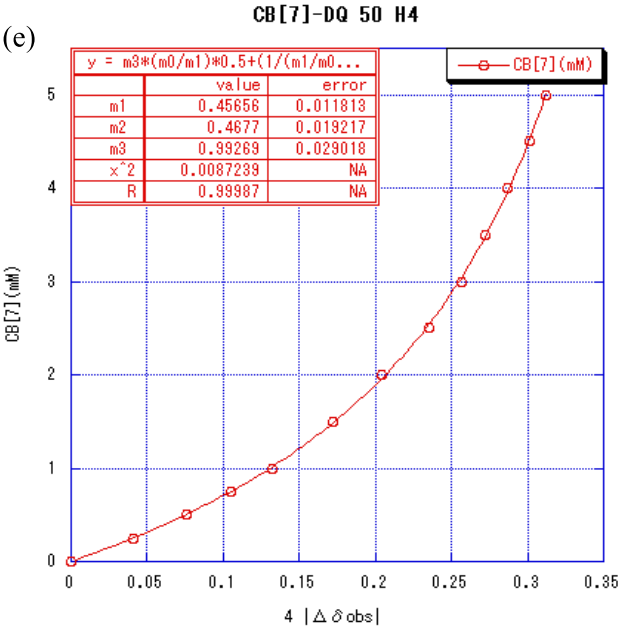
CB[7]-DQ 50 H4
y = m3*(m0/m1)*0.5+(1/(m1/m0...
CB[7](mM)
value error
m1 0.45656 0.011813
m2 0.4677 0.019217
m3 0.99269 0.029018
x^2 0.0087239 NA
R 0.99987 NA
CB[7](mM)
4 |Δδobs|

(f)

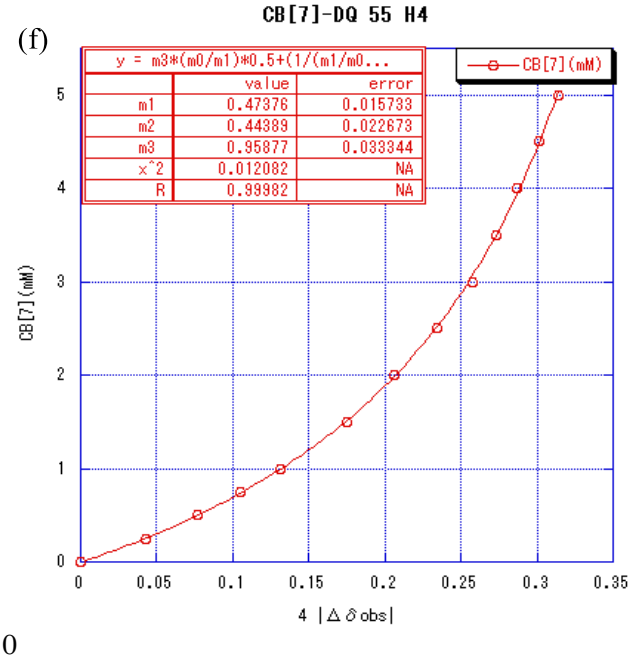
CB[7]-DQ 55 H4
y = m3*(m0/m1)*0.5+(1/(m1/m0...
CB[7](mM)
value error
m1 0.47376 0.015733
m2 0.44389 0.022673
m3 0.95877 0.033344
x^2 0.012082 NA
R 0.99982 NA
CB[7](mM)
4 |Δδobs|

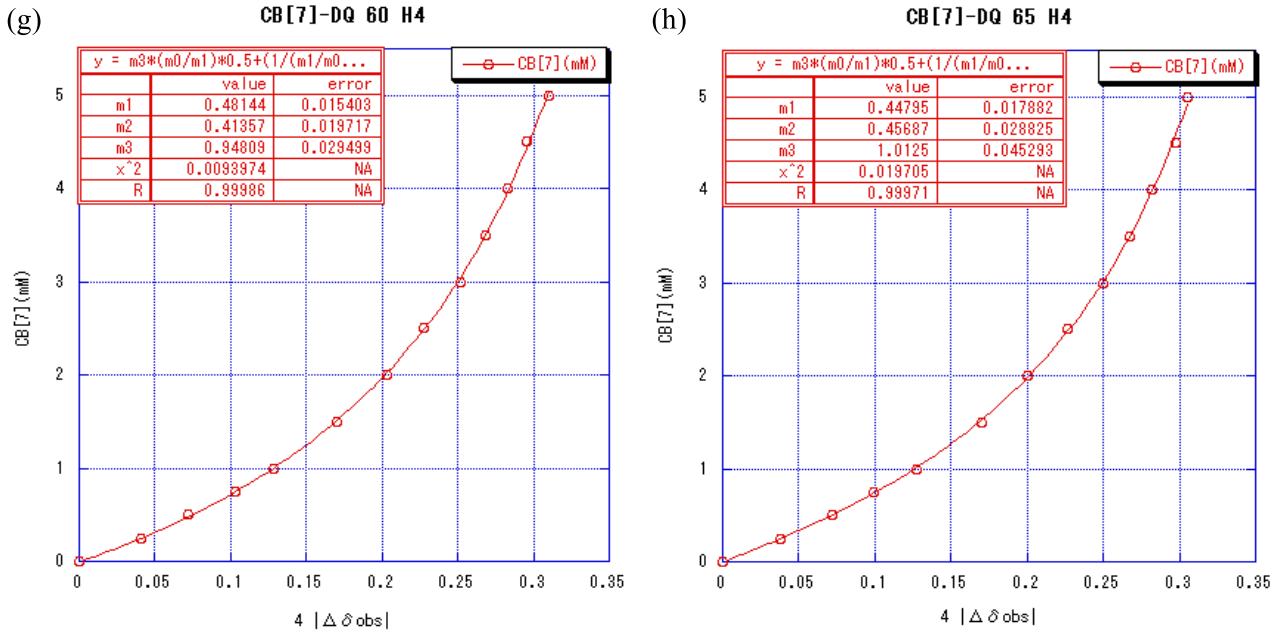

Fig. S8 Regression analysis by using Eqn (1) based on $\Delta\delta_{obs}$ of the H^4 proton signal of DQ (0.5 mM DQ) at 30 – 65 °C in NaCl-D_2O: (a) 30 °C, (b) 35 °C, (c) 40 °C, (d) 45 °C, (e) 50 °C, (f) 55 °C, (g) 60 °C, and (h) 65 °C.

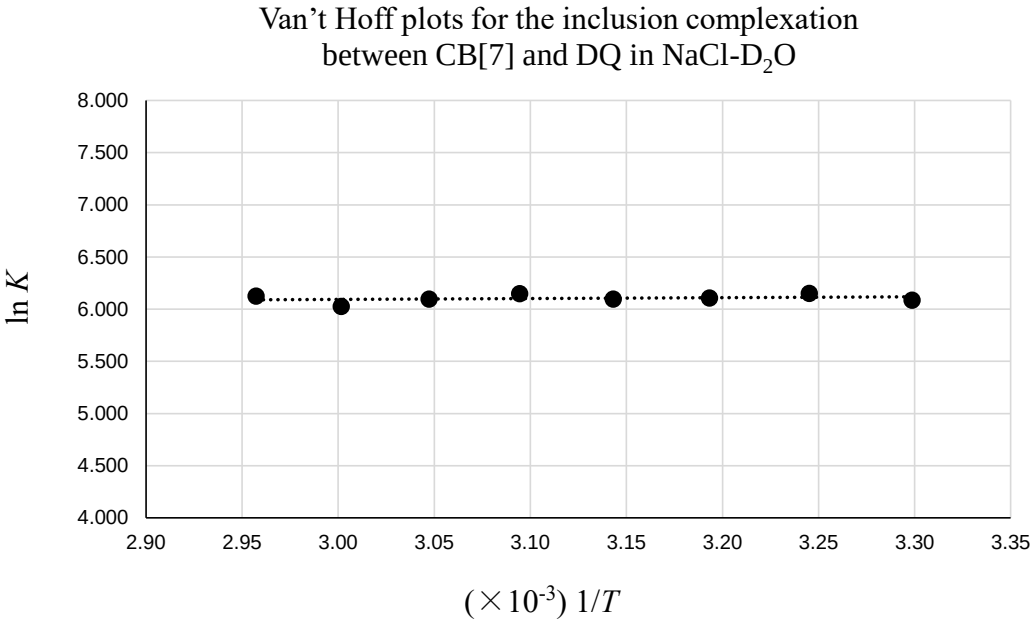

Fig. S9 Van't Hoff plots for the inclusion complexation between CB[7] and DQ (0.5 mM DQ) in NaCl-D_2O.

The association constant for the inclusion complexation of CB[7] and DQ was calculated via Benesi-Hildebrand method in pD1.2, pD7.4, and NaCl-D_2O while continuously increasing the CB[7] concentration ([CB[7]) from 0 to 5 mM in a constant concentration of DQ ([DQ]; 0.05 mM). The UV spectroscopy was conducted by using a UVmini-1240 (SHIMADZU, Japan); the absorbance was recorded at 330 nn and 35 °C. The following Eqn (2) was used for regression analysis. K is the association constant of CB[7] and DQ, ΔE means ($A_{obs} - A_{DQ}$), $\Delta\varepsilon$ indicates ($\varepsilon_{complex} - \varepsilon_{DQ}$), and A_{obs} and A_{DQ}, $\varepsilon_{complex}$ and ε_{DQ} are the absorbance of CB[7]-DQ mixture and DQ in a free state, and the molar absorption coefficient of the CB[7]-DQ inclusion complex and DQ in a free state.

$$\text{CB[7]} + \text{DQ} \underset{}{\overset{K}{\rightleftharpoons}} \text{CB[7]-DQ}$$

$$\frac{1}{\Delta E} = \frac{1}{K\,\Delta\varepsilon\,[\text{DQ}][\text{CB[7]}]} + \frac{1}{\Delta\varepsilon\,[\text{DQ}]} \quad \cdots\cdot \text{Eqn (2)}$$

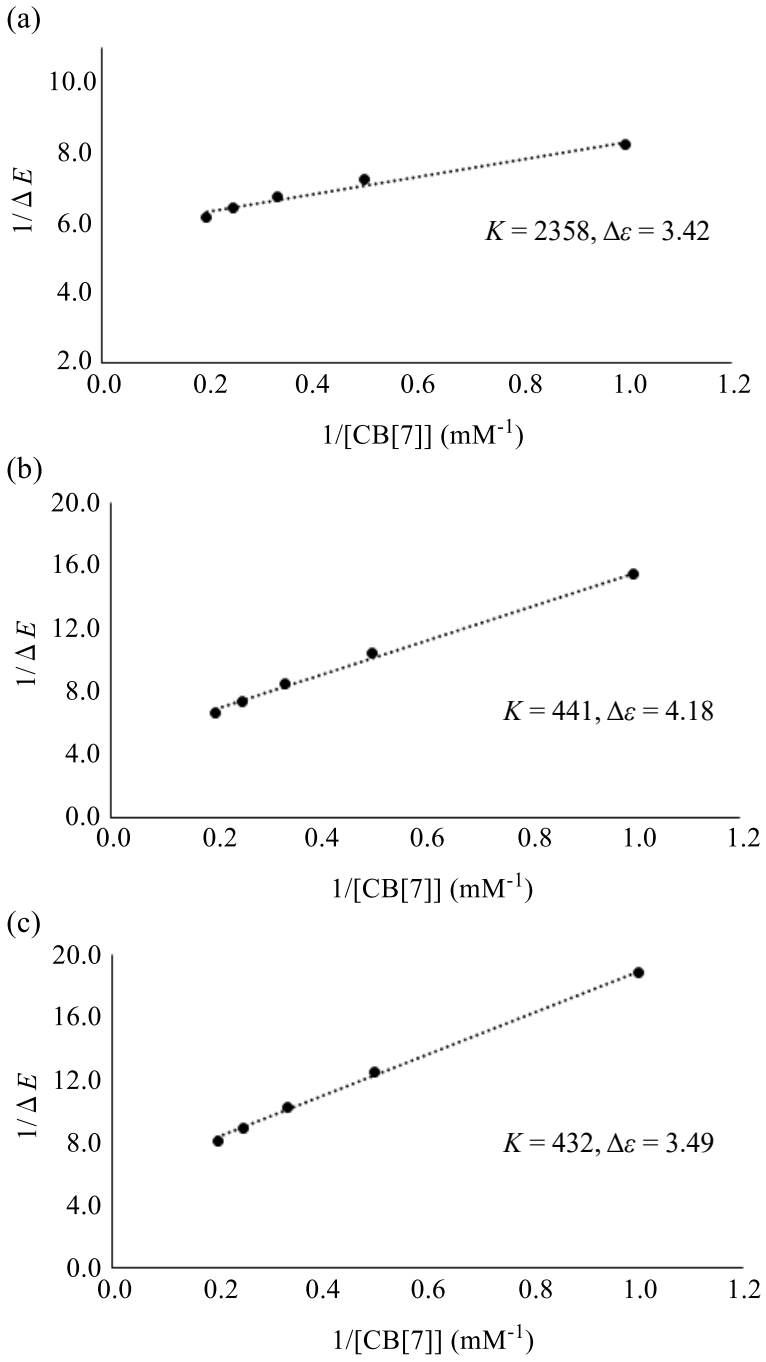

Fig. S10 Regression analysis by using Eqn (2) based on ΔE at 35 °C in (a) pD1.2, (b) pD7.4, and (c) NaCl-D_2O.

The *n* and *K* for the complexation between CB[7] and DQ were calculated via regression analysis by using Eqn (1) at 30 - 65 °C in NaCl-D_2O. The CB[7] concentration continuously was increased from 0 to 10 mM in a constant concentration (1 mM DQ). The ΔG, ΔH, and ΔS for the inclusion complexation of CB[7] and DQ were derived from Van't Hoff plots by using association constants. The association constant at 35 °C was 484 M^{-1}, and ΔG, ΔH, and $T\Delta S$ were －15.8 kJ/mol, －1.1 kJ/mol and －14.7 kJ/mol, respectively.

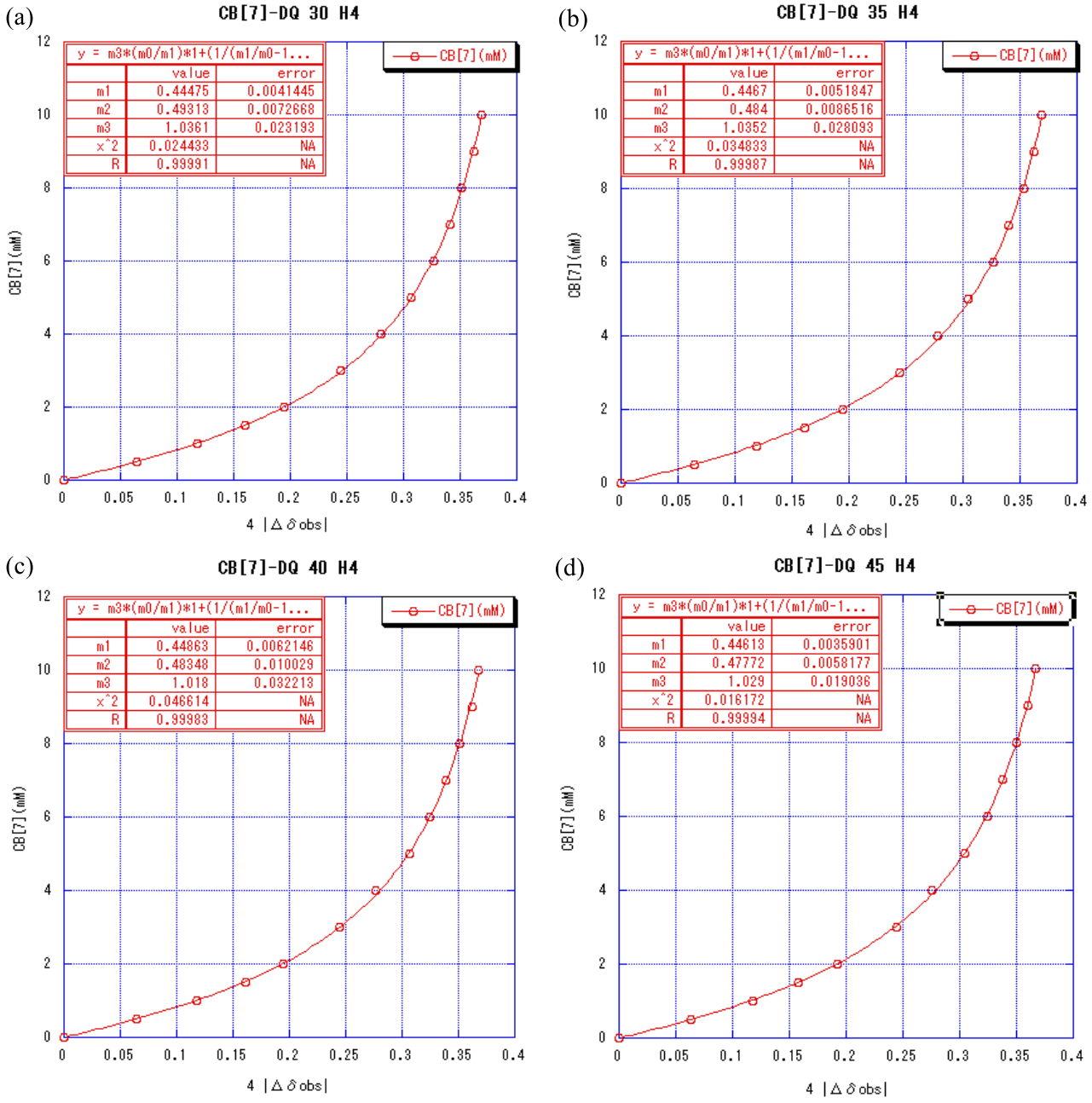

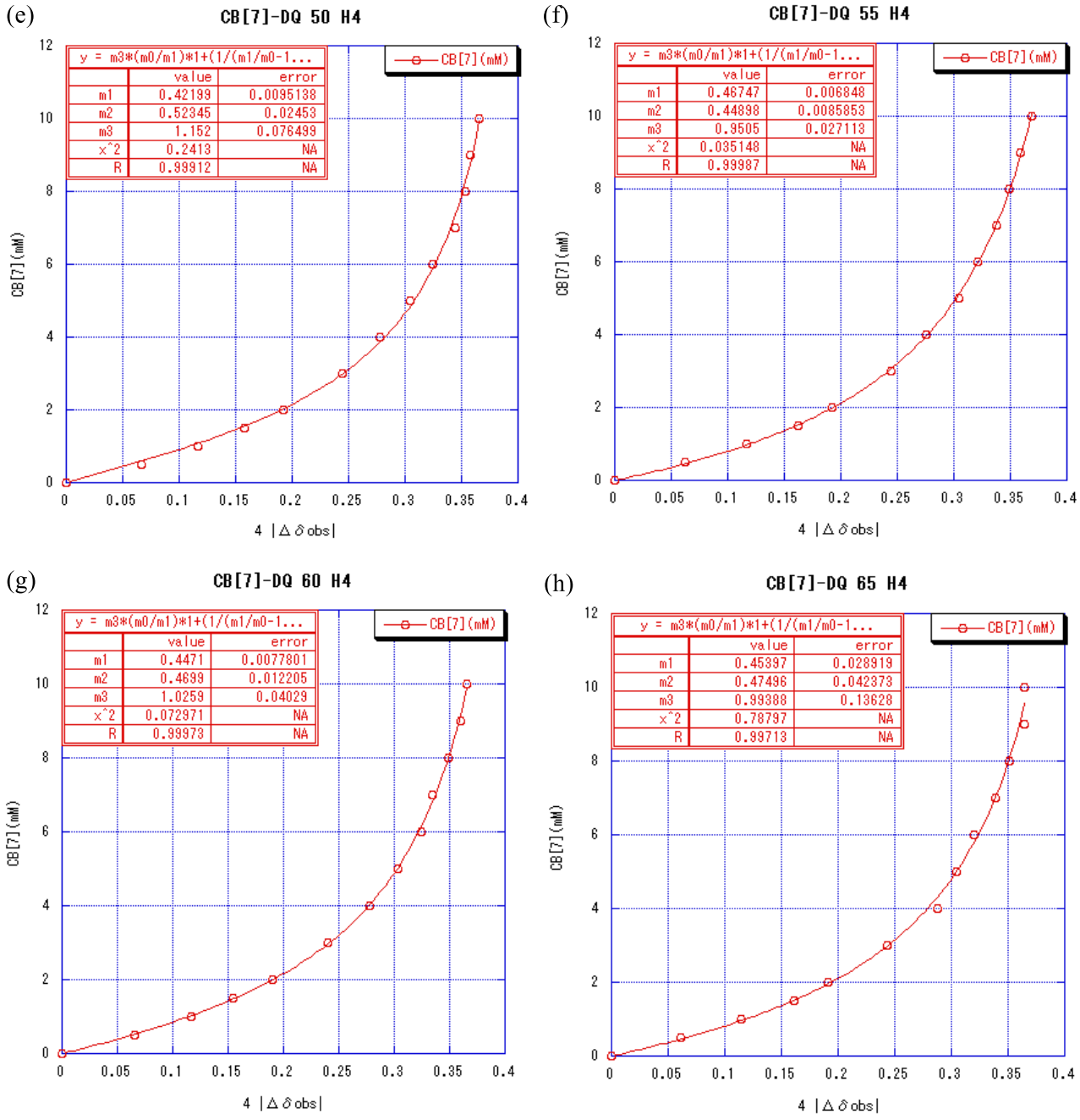

Fig. S11 Regression analysis by using Eqn (1) based on $\Delta\delta_{obs}$ of the H^4 proton signal of DQ (1 mM DQ) at 30 - 65 °C in NaCl-D_2O: (a) 30 °C, (b) 35 °C, (c) 40 °C, (d) 45 °C, (e) 50 °C, (f) 55 °C, (g) 60 °C, and (h) 65 °C.

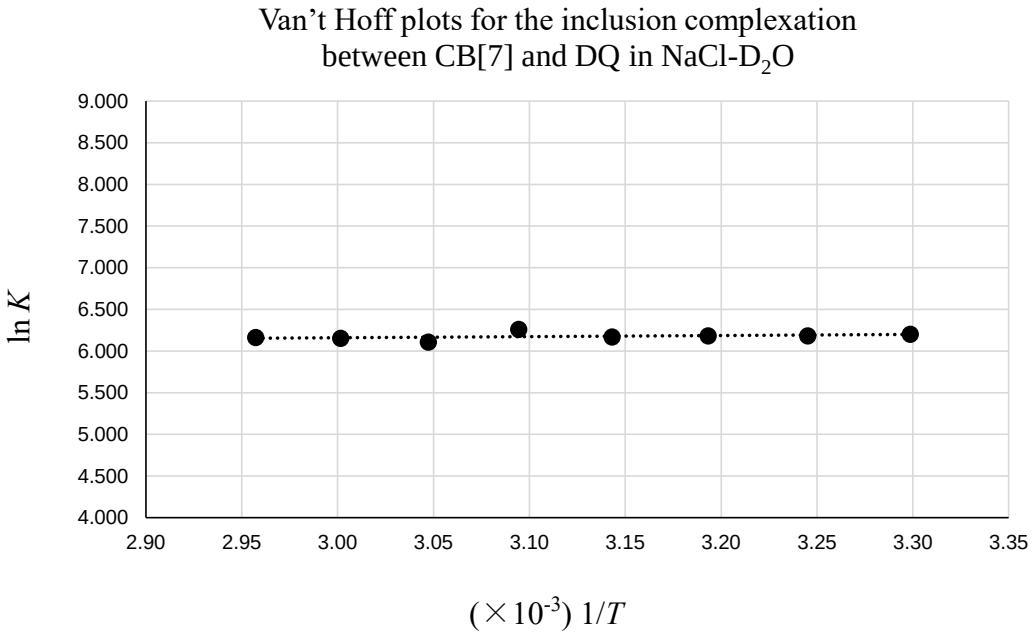

Fig. S12 Van’t Hoff plots for the inclusion complexation between CB[7] and DQ (1 mM DQ) in NaCl-D_2O.

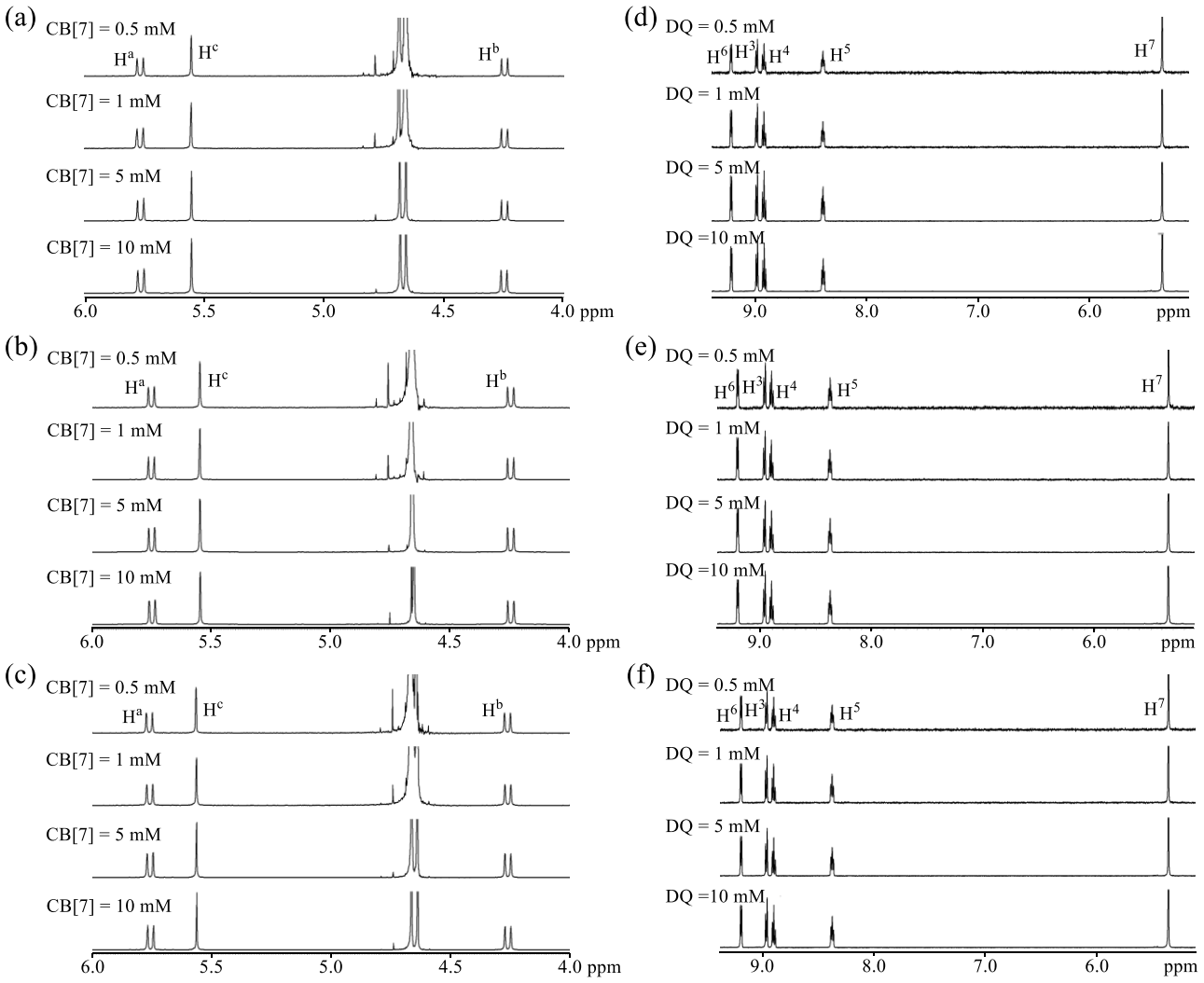

Fig. S13 Behavior of CB[7] or DQ, as revealed via ^{1}H NMR when increasing the CB[7] or DQ concentrations in pD1.2, pD7.4, and NaCl-D_2O: CB[7] in (a) pD1.2, (b) pD7.4, and (c) NaCl-D_2O; DQ in (d) pD1.2, (e) pD7.4, and (f) NaCl-D_2O. H^a, H^b, and H^c indicate the proton signals of CB[7]. H^3, H^4, H^5, and H^6 indicate the proton signals of DQ.

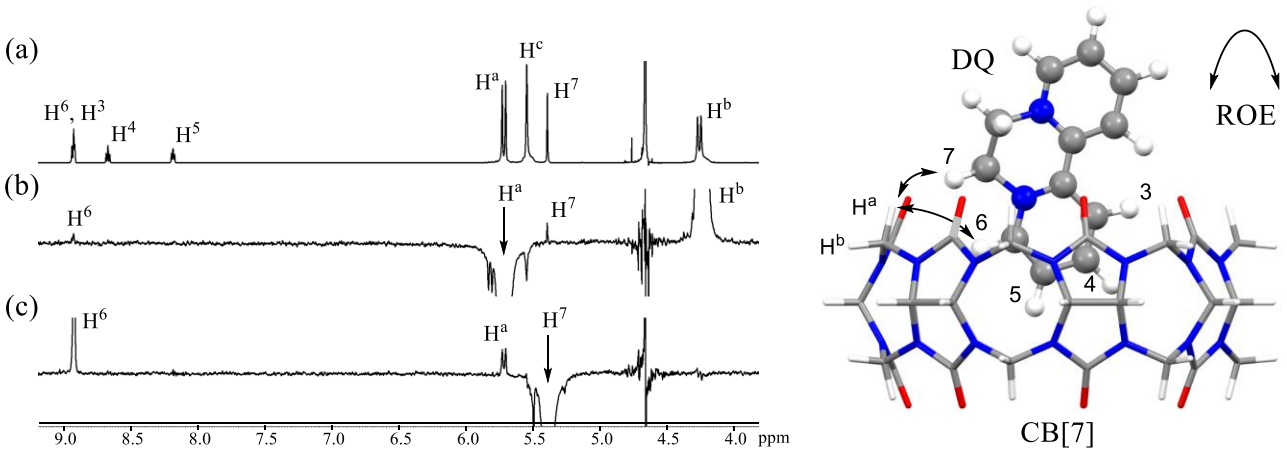

Fig. S14 Rotating-frame Overhauser effect (ROE) observed between CB[7] and DQ when forming the inclusion complex in pD7.4: (a) ^{1}H NMR spectrum of CB[7] and DQ; (b) one-dimensional (1D) ROESY spectrum irradiated to the H^{a} proton of CB[7]; (c) 1D ROESY spectrum irradiated to the H^{7} proton of DQ. The half-arrows in 1D ROESY spectra indicate positions of the irradiated proton signals.

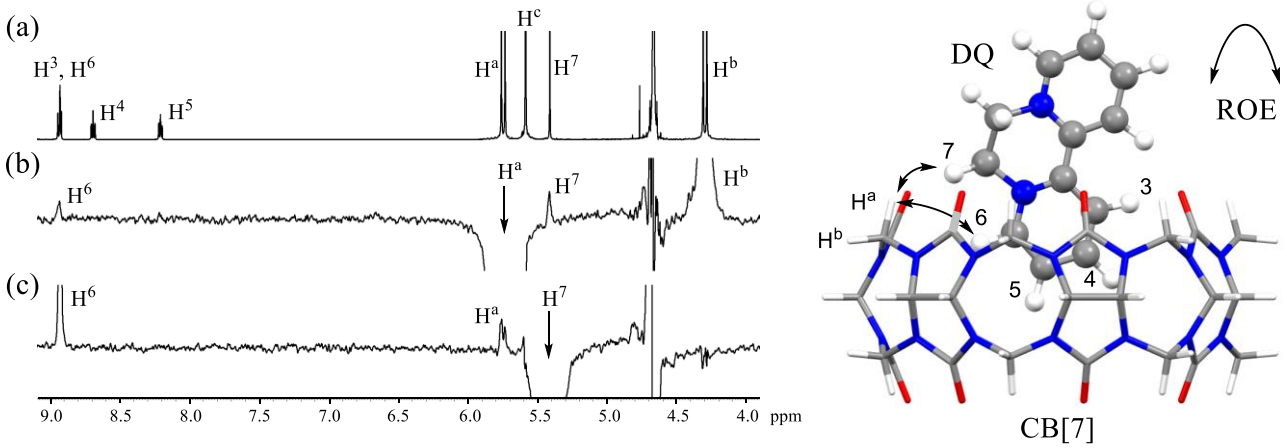

Fig. S15 ROE observed between CB[7] and DQ when forming the inclusion complex in NaCl-D_2O: (a) ^{1}H NMR spectrum of CB[7] and DQ; (b) 1D ROESY spectrum irradiated to the H^{a} proton of CB[7]; (c) 1D ROESY spectrum irradiated to the H^{7} proton of DQ. The half-arrows in 1D ROESY spectra indicate positions of the irradiated proton signals.